JOURNAL OF NUCLEAR MEDICINE 8:1-24, 1967

The ACRH Brain Scanning System

R. N. Beck, D. B. Charleston, P. Eidelberg and P. V. Harper[1]

Chicago, Illinois

INTRODUCTION

The feasibility of using radioisotope scanning systems to detect a variety of brain lesions has been recognized for a number of years and the use of this procedure on a routine basis has gradually increased. The fact that several well-established methods for locating intercranial lesions already exist, such as angiography, pneumoencephalography and electroencephalography, has not hindered this development, since each of these methods has well-known limitations and undesirable features. The lack of widespread enthusiastic acceptance of brain scanning is due more to the cumbersome and time-consuming nature of the procedure. To keep the radiation dosage to the patient below the maximum permissible level, only relatively small quantities of iodine-131, the first and most commonly used isotope, can be used. In addition, collimated detectors for the 364 keV γ-rays from this isotope are relatively inefficient. As a result, the time required for brain scanning is long, usually one to three hours if scans are to include more than one view of the head. Furthermore, the spatial resolution is exceedingly poor by x-ray standards.

We reviewed the problem of brain scanning at a time when several approaches to the imagining of distributions of high energy photons had already been introduced. The pioneering work of Cassen (1) had stimulated the development of what are now regarded as "conventional scanners" consisting of single scintillation detectors responding to single photons; Brownell (2) had successfully demonstrated the use of a "positron scanner" consisting of two detectors that responded to coincident photons from positron annihilation; Anger (3) had succeeded in developing a stationary scintillation detector or "γ-ray camera" that viewed the entire region of interest simultaneously. Each of these approaches required serious consideration because each approach was capable of further development. This fact has subsequently been shown by the introduction of a highly efficient hemispherical collimator by Cassen (4); the ingenious use of conventional detectors in a novel scanning mode producing cross section images,

[1]The Argonne Cancer Research Hospital operated by the University of Chicago for the United States Atomic Energy Commission.

by Kuhl (5); the adaptation of the camera system to positron emitters by Anger (6); the development of a digital version of the Anger camera by Bender and Blau (7); and the recent use of image intensifiers by Kellershohn (8) and Ter-Pogossian (9).

This paper describes a multi-detector brain scanner that represents our attempt to improve systems of the conventional, rectilinear moving detector type. Any attempt to improve the brain scanning procedure must consider both physical and biological parameters. On the physical side, a theoretical study (10, 11) of detector sensitivity and tumor contrast as function of γ energy indicates that, under typical conditions, gamma-rays in the energy range of 100-200 keV are optimum[1] for detecting midline tumors. On the biological side, the isotope must be taken up in different concentrations by the tumor and normal tissues, and the radiation dosage to the patient should be minimal.

These considerations stimulated the search for a more suitable γ emitter, which led to the introduction of technetium-99m (11). This isotope is produced by the β^- decay of molybdenum-99 from which it is easily separated and prepared for injection (13, 14). The metastable ^{99m}Tc subsequently decays by an isomeric transition, with the emission of a 140 keV γ-ray, to Tc, which is essentially stable (2.2×10^5 year half-life). Since the half-life of ^{99m}Tc is short (6 hours) and the material is essentially a pure γ emitter (only about 7% of the 140 keV γ's are internally converted), the radiation dosage per injected μCi is very low compared with that from iodine-131.

The ACRH brain scanner, shown in Fig. 1, was a concurrent development. Briefly, the system consists of four collimated scintillation detectors, arranged in opposing pairs, which simultaneously scan the patient's head. Pulses from these detectors are fed to four pulse height analyzers adjusted to accept only photopeak pulses for recording. The recording system consists of four light projectors which move with the detectors and produce a bell-shaped spot on film for each selected photopeak pulse. Count rate meters monitor each channel, but are not used for contrast enhancement or background erase.

When used with a 10 mCi intravenous injection of ^{99m}Tc, the ACRH brain scanner can produce simultaneous lateral photoscans of conventional quality in approximately one minute, although the scanning time is usually extended to about 10 minutes to produce pictures of superior quality. This quantity of ^{99m}Tc as pertechnetate produces a whole-body radiation dosage of approximately 100 mr, the critical organ being the stomach, which receives approximately 3 rads. Although spatial resolution is still poor by X-ray standards, this system employs

[1]The term "optimum" is used in the mathematical sense to refer to that γ energy which, for a specified set of assumed physical conditions, maximizes a certain criterion called the "normalized figure of merit," a quantity inversely proportional to the time required to resolve the tumor and normal count rates statistically (10). For a different criterion or a different set of physical conditions, a different "optimum" energy would be obtained. The study referred to above designed for a 2″ × 2″ NaI (Tl) crystal, with lead collimators having a 4″ focal length, 1″ diameter of view, to detect a 1″ diameter midline tumor having an uptake ratio of 2:1. For equal numbers of γ's produced per cm^3-sec in the tissue, it appeared (11) that the optimum γ energy is 100 keV. This study did not deal with scattered radiation. When scatter is taken into account, the optimum γ energy is somewhat higher (12).

collimators having a smaller radius of view than is ordinarily used for brain scanning. The ACRH brain scanner has been used with ^{99m}Tc since August, 1963. Some of its features were first demonstrated on a prototype small-animal scanner (15).

THE IDEAL IMAGING SYSTEM

Since the distribution of radioactive material in the brain is a volume distribution, an ideal imaging system would produce a three-dimensional image. As yet, such systems have not been devised, although the cross section scanner of Kuhl (5) has demonstrated their feasibility and Harper (16) has discussed a possible realization. A (hypothetical) ideal system of the general type described here would produce an exact image of an attenuated normal projection of the volume distribution onto a plane. This can be described as follows: If $\rho(x,y,z)$ specifies the concentration of γ activity,[1] an attenuated normal projection onto the (X-Y) plane is given by

$$\sigma(x,y) = \int_0^\infty \rho(x,y,z)e^{-\mu z}dz \qquad (1)$$

where z is the depth below the surface of the head, and μ is the attenuation coefficient in the tissue. In practice, we do not observe a perfect image of the projected distribution; rather, the observed image differs from $\sigma(x,y)$ in a variety of ways which may be described as artifacts due to the limitations of the scanning system.

ARTIFACTS AND THEIR REDUCTION

Our approach to designing the ACRH brain scanner might be described as an attempt to minimize artifacts inherent in systems of this type, without increasing the scanning time, radiation dosage, etc. Certain aspects of this approach are described in more detail in reference (17). The following artifacts were considered:

A. *Statistical Structure:* When a collimated scintillation detector scans a source characterized by its equivalent sheet distribution $\sigma(x,y)$, the true mean count rate due to properly collimated γ's is given approximately[2] by

$$C(x,y) = G\,\eta\Psi\sigma(x,y) \qquad (2)$$

---

[1] In this formulation, ρ has dimensions $\left[\frac{\gamma\text{'s produced}}{\text{sec-cm}^3}\right]$ and can be expressed in terms of the tracer efficiency, $k\left[\frac{\gamma\text{'s produced}}{\text{sec-cm}^3\text{-rad}}\right]$, and the permitted radiation dosage to the whole body or to a critical organ, d[rads]; that is, $\rho = kd$. The projection of ρ, namely $\sigma(x,y)$, has dimensions of $\left[\frac{\gamma\text{'s produced}}{\text{sec-cm}^2}\right]$

[2] Equation (2) holds precisely only when $\sigma(x,y)$ is uniform over the collimator field of view; thus, for a highly non-uniform source, equation (2) holds precisely only when the width of the field of view is "infinitely small." The effect of finite spatial resolution on $C(x,y)$ is discussed in section B2.

where $G(cm^2)$ is the geometrical efficiency[1] of the collimator for responding to activity on a sheet distribution, η is the photopeak crystal efficiency, and Ψ is the "window efficiency," or the fraction of photopeak pulses selected by the pulse height analyzer.

If $t\left[\frac{sec}{cm^2}\right]$ is the time spent by the detector per unit area, the true mean count rate gives rise to the true mean image[2] of the source defined by

$$N(x,y) = C(x,y)t \tag{3}$$

where $N(x,y)\left[\frac{counts}{cm^2}\right]$ is the true mean number of γ's which would be detected per unit area, if the scan could be repeated many times.

On this basis, the ideal image of a uniform source [$\sigma(x,y)$ = constant] is a uniform image [$N(x,y)$ = constant]. In practice, the observed number of counts per unit area is not constant, but varies randomly to produce a non-uniform or "structured" image. If N is the true mean number of counts per unit area, then the observed number, being Poisson distributed, will vary randomly about N with a standard deviation $\sigma_N = \sqrt{N}$, or a fractional standard error $\epsilon = \frac{\sigma_N}{N} = \frac{1}{\sqrt{N}}$. The magnitude of ϵ can be used as a measure of this random structure which approaches 0 as N approaches ∞. [Rossmann (20) has described a related, but more complex structure, called quantum mottle, which depends not only on N but also on the shape of the recorded spots]. The origin of this structure is therefore described as statistical fluctuation which can be reduced only by increasing the number of properly collimated γ's recorded per unit area. Despite the use of high scan speeds, this artifact is reduced in the ACRH system in the following ways:

1) High count rates result from the choice of ^{99m}Tc which can be administered in large quantities.
2) Four detectors scan the head simultaneously (Fig. 1).

The axes of the upper and lower detectors are separated by 4½″ so that a 9″ region is scanned when the detectors index vertically 4½″. A selector switch enables the operator to perform the scan with either the lower detectors, the upper detectors, or all four.

Two sets of detectors have been constructed for this system. The original set consisted of NaI(Tl) crystals, 3⅜″ by 1¾″, integrally mounted on EMI9531B photomultiplier tubes. (Fig. 2.) This crystal thickness was considered adequate for γ's up to ^{131}I radiation (364keV). The new detectors are similar, except for the crystal thickness, which is ½″. This is adequate for γ's below 200 keV.

3) Detector sensitivity can be maximized by making the septa of focused collimators just thick enough to reduce unwanted septal penetration to a negli-

---

[1]In previous papers (10, 11, 18) the symbol E has been used to denote this geometrical property of the collimator, which is similar to Brownell's (19) "slab efficiency," $G_s \cong g_o d^2$.

[2]In what follows, we use the term "image" to refer to either $C(x,y)$ or $N(x,y)$ since they differ only by a constant factor t.

gible level. (Figs. 3 and 4.) For a given penetration fraction, the required septum thickness increases with γ energy, so that focused collimators designed for 140 keV (^{99m}Tc) are about twice as efficient as similar collimators designed for 364 keV ^{131}I).

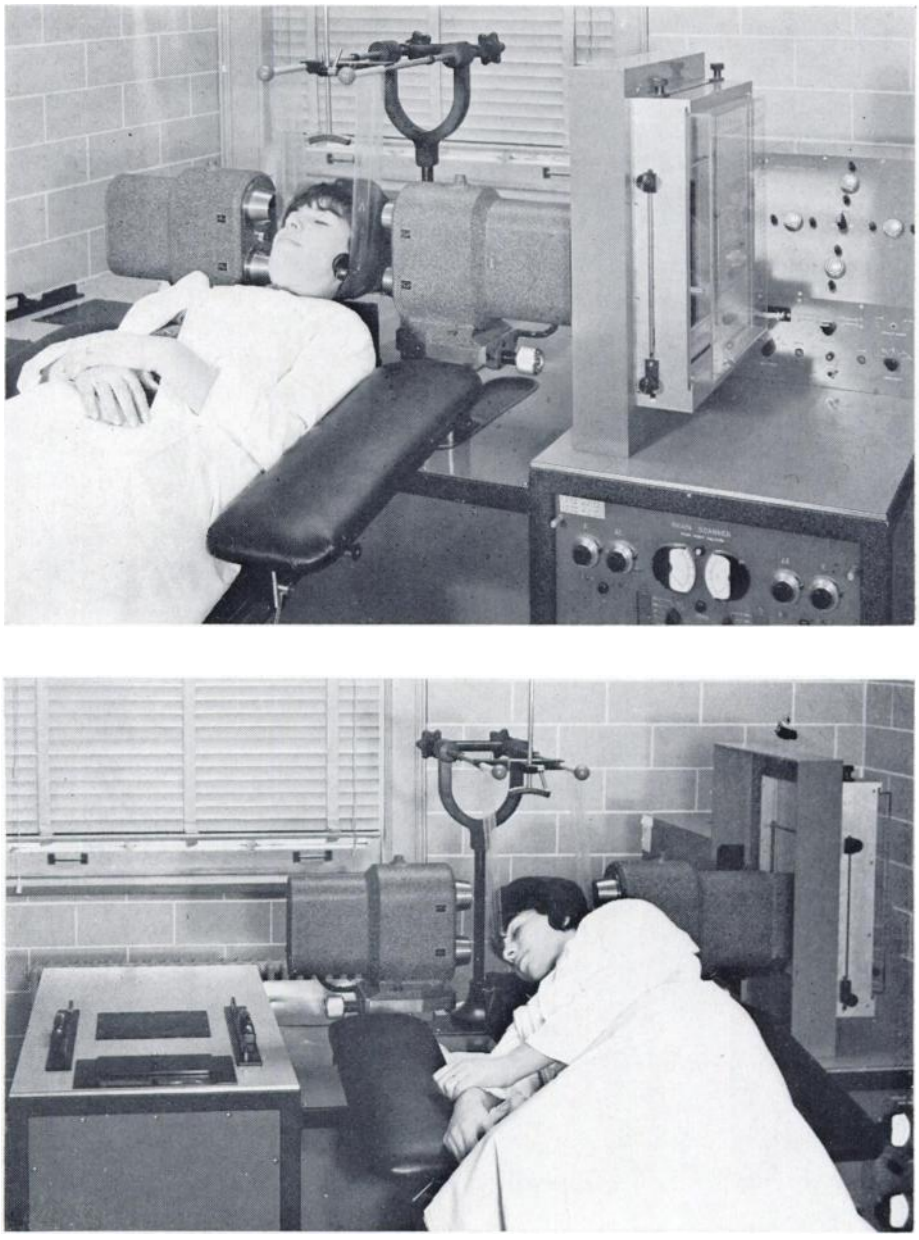

Fig. 1. The ACRH Brain scanner consists of four scintillation detectors arranged in opposing pairs, each detector having an associated pulse height analyzer and pulsed light projector. Scan information is recorded on two sheets of film, one for each side of the head.

4) An interrupted light beam system is used to minimize the time spent in scanning beyond the patient's head so that the detectors are over the region of interest during a large fraction of the scanning time.

In the center holes of the collimators on the patient's left are small focused light bulbs whose beams indicate the positions of the collimator axes and aid in positioning the patient. In the center holes of the opposite collimators are IN2175 photodiodes which produce signals when the light path is closed by scanning beyond the patient's head. This system is used to reverse the direction of scan so as to minimize the time spent in scanning beyond the head. In addition, this system is used to record an outline of the head on the film. This is accomplished by four light projectors (Fig. 6) consisting of single Amperex 6977's which are pulsed by signals from the photodiodes to produce small, intense outline marks on the film. These projectors may also be pulsed manually by a push button switch to produce "land marks" on the film.

B. *Reduced Contrast:* When the distribution of activity is not uniform [$\sigma(x,y) \neq$ constant], the true mean count rate gives rise to structures in the image which are neither as prominent nor as sharply outlined as the corresponding structures in the object. This can be formulated quantitatively as follows: Let σ_t be the source strength over a tumor region that is small compared to the entire source, the latter being otherwise normal with a uniform strength σ_0. The lack of uniformity in the tumor and normal regions could be measured by the arithmetic difference ($\sigma_t - \sigma_0 \neq 0$); the fractional difference $\left(\frac{\sigma_t-\sigma_0}{\sigma_0} \neq 0\right)$; the ratio $\left(\frac{\sigma_t}{\sigma_0} \neq 1\right)$; or by a somewhat less familiar quantity called the contrast or modulation, and defined by

$$m_0 = \frac{\sigma_t-\sigma_0}{\sigma_t+\sigma_0}. \tag{4}$$

Using the latter measure, this "object structure" gives rise to "image structure" which is also measured by its contrast or modulation defined by

$$m_i = \frac{C_t-C_0}{C_t+C_0}. \tag{5}$$

TABLE I

TABLE OF CLINICAL RESULTS FOR THE FIRST 182 PATIENTS SCANNED.

Category	*Definite*	*Probable*	*Total*
Positive	63	5	68
Negative	78	10	88
False positive	2	4	6
False negative	8	2	10
Technically unsatisfactory			10
			182

We can go one step further and introduce a quantity called the modulation transfer function (MTF) defined by

$$m_i = (MTF)m_o \text{ or } MTF = \frac{m_i}{m_o} \tag{6}$$

The MTF measures the degree to which contrast or modulation in the object is transferred to the image by the scanning system.

If the detector responded only to properly collimated γ rays, and, in addition, had perfect spatial resolution, then equation (2) could be used to compute the count rates in equation (5). Under these conditions the image contrast would be a perfect replica of the object contrast; that is, $m_i = m_o$ and MTF = 1.

Equation (2), however, should be interpreted as describing a theoretical ideal not realized by actual systems, which always transmit object contrast to the image imperfectly; thus, for actual systems, $m_i < m_o$ or MTF < 1[1]. The phenomena responsible for contrast reduction can be separated into two categories: 1) uncollimated radiation, which reduces contrast uniformly over large areas, and 2) finite spatial resolution of the collimator, which results in local smoothing and greatly reduces image contrast for small structures.

[1]The image may be recorded by a nonlinear system using circuits for contrast enhancement so that the contrast in the recorded image may exceed m_o. Circuits of this type are built into this scanner for research purposes, but are not used for patient scanning.

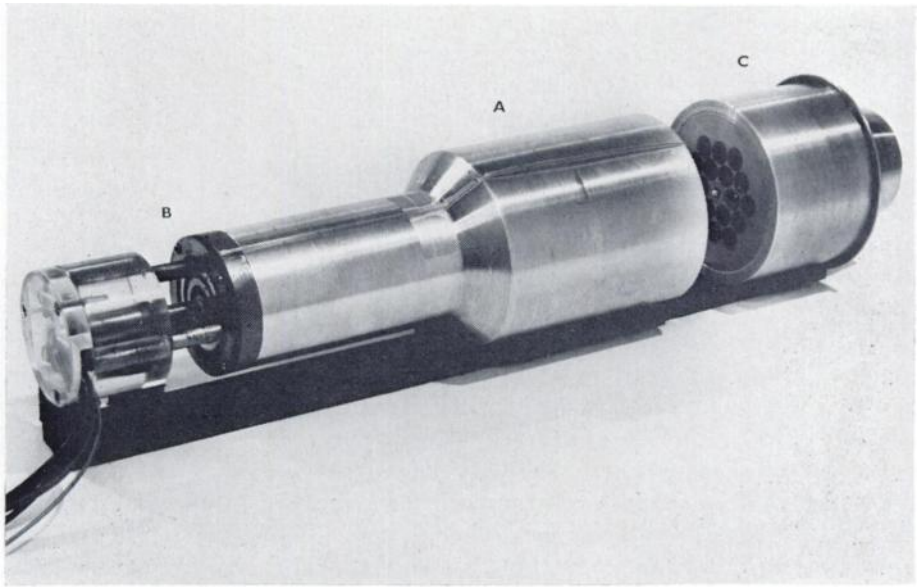

Fig. 2. Each detector consists of a NaI(Tl) crystal and photomultiplier tube, integrally mounted (A). Electrical contact to concentric rings is made by spring-loaded electrodes (B) which can retract 1″ to allow for collimators (C) of varying thickness. A light bulb (photodiode) is mounted in the center hole of each collimator on the patient's left (right).

1) Detector response to uncollimated radiation.

a) Background or noise: Even when $\sigma(x,y) = 0$, the observed count rate is not zero. This is due to a combination of cosmic radiation, nearby radioactive sources, natural radioactivity in the materials of the radiation detectors, etc.

In the brain scanner, the background count rate is reduced by the use of NaI(Tl) crystals that are just thick enough to achieve high photopeak efficiency for the γ energy used. Background is further reduced by lead shields for these crystals, and pulse height analyzers that select only the useful portion of the pulse amplitude spectrum. Shields of 2″ lead (for the original 1¾″ crystals) have been replaced by much lighter, ½″ shields (for the ½″ crystals) which are adequate for γ's below 200 keV.

b) Septum penetration: Since most of the γ's that enter the detector by penetrating the collimator septa originate outside the geometrical field of view, they are essentially uncollimated and do not contribute to the formation of a structured image. For this reason, the penetration fraction, P, is one of the most important quantities considered in collimator design. It is controlled by the choice of septum thickness for a specific γ energy, collimator material, crystal diameter, radius of view, and focal length (18). If the septa are too thick, collimator efficiency is needlessly reduced; if too thin, excessive penetration reduces contrast. In all collimators designed for ^{131}I, ^{203}Hg and ^{99m}Tc, the penetration fraction has been kept below 0.1. Figures 3 and 4 show collimators designed for ^{99m}Tc and ^{203}Hg respectively. Figure 4 shows marked contrast (MTF) reduction for ^{131}I due to septum penetration.

c) Scattered radiation: Gammas that enter the detector from outside the collimator field of view, by Compton scattering in the tissue, also reduce image contrast. Since scattered photons have less energy than the unscattered γ-rays, some of the scattered radiation can be rejected by use of pulse height analyzers (PHA's). Because scintillation detectors have imperfect energy resolution, the pulse amplitude spectra due to scattered and unscattered photons overlap. As a consequence, not all scattered photons can be rejected by PHA's without seriously reducing the counting efficiency for unscattered γ-rays. A base line discriminator setting is needed which achieves an optimum compromise between rejection of scattered photons and the recording of unscattered γ-rays. If the optimum base line setting is defined as that setting which maximizes the above mentioned figure of merit (10,12), then the optimum setting is a function of the γ energy, the energy resolution of the detector, and the source size. For example, the optimum setting for a uniform distribution of ^{99m}Tc in a brain phantom 16 cm in diameter is $\sim$ 125 keV for a detector having 16% resolution at 140 keV (12).

Taking the above responses into account, the total response of the detector can be thought of as the sum of responses to collimated and uncollimated radiation, and equation (2) can be modified as follows: When the detector is over a normal region where the source strength is σ_o, the total count rate can be written

$$C_o = G\eta\Psi\sigma_o(1 + P + S) + B \qquad (7)$$

where P and S are the penetration and scatter fractions (21), respectively, and B is the background count rate. When the detector is over a tumor region, where

the source strength is σ_t, the situation is somewhat more complex. In this case, we assume that the tumor is large enough to cover the geometrical field of view uniformly, but not much larger. Thus the response to properly collimated γ's is $G\eta\Psi\sigma_t$. Since, however, most of the γ's which enter the detector by septum penetration or by scattering in the source originate outside the collimator field of view, where the source strength is σ_o, the count rate due to penetration and scatter is still approximately $G\eta\Psi\sigma_o(P+S)$. The total count rate over the tumor region is therefore

$$C_t = G\eta\Psi[\sigma_t + \sigma_o(P + S)] + B \tag{8}$$

When equations (7) and (8) are used in equation (5) to compute the image contrast, that quantity is reduced to

$$m_i = \frac{G\eta\Psi(\sigma_t - \sigma_o)}{G\eta\Psi[\sigma_t + \sigma_o + 2\sigma_o(P+S)] + 2B} \tag{9}$$

From this equation it is clear that image contrast is reduced by all three forms of uncollimated radiation; therefore, in general, $m_i < m_o$ or MTF < 1.

2) Finite resolution of the collimator.

Even when we assume that background, penetration, and scattered radiation are all negligible, the image contrast is still, in general, less than the object contrast to a degree that depends on the size of the object structure relative to the width of the collimator field of view. For structures that are very large compared to the field of view (this means that the source, $\sigma(x,y)$, is essentially uniform over the field of view), equation (2) is a very good approximation, and the image contrast is very nearly equal to the object contrast. On the other hand, when structures in the object are much smaller than the width of the field of view (this means that the source, $\sigma(x,y)$, is non-uniform within the field of view), equation (2) no longer holds and image contrast is much smaller than object contrast. As a result, the image is a smoothed version of the object, and very small structures may be lost entirely. (If P, S, and B are not zero, then the contrast is, of course, even further reduced.)

To compute the geometrical response to small structures, equation (2) must be replaced by a more general formulation that takes into account the collimator sensitivity to activity at each point within the field of view. The function describing this sensitivity is called the point source response function (abbreviated psrf), $p(x,y,z)$, and is proportional to the solid angle of view, $\Omega(x,y,z)$, through the collimator from the point (x,y,z) at which a γ-ray is emitted. This solid angle is greatest for points on the collimator axis and decreases to zero at the periphery of the field of view. The shape of this function changes with distance from the collimator. Near the collimator face it tends to be uniform or flat-topped, while at the focal distance it tends to be quite peaked and almost conical. At intermediate distances it is bell-shaped and approximately Gaussian.

The total response to an arbitrary source, $\rho(x,y,z)$, is then found by summing the product of the sensitivity function over the source distribution, taking exponential attentuation with depth, z', into account

$$C(x,y) = \eta\Psi\int_v p(x'-x,y'-y,z'+z_0)\rho(x',y',z')e^{-\mu z'}\,dx'dy'dz'. \qquad (10)$$

Here, z_0 is the clearance between the collimator face and the tissue surface. While this formulation is general enough for most applications, it is too complex to be very useful.

If we put aside the problem of computing C(x,y) precisely, the description of collimator response by p(x,y,z) can be simplified conceptually by considering the average magnitude of this function (at a given z) to represent the collimator sensitivity, and the shape of the function to determine the spatial resolution. The description can be further simplified mathematically by defining the spatial resolution as the full width of p(x,y,z) at its half-maximum height. This amounts to replacing the two-dimensional function p(x,y) at each distance z, by two numbers that denote the sensitivity and spatial resolution. While this simplification eliminates the possibility of computing C(x,y) precisely, it would appear that we can still compare the quality of collimators in terms of this definition of resolution; thus, we would expect to observe the best scans from the collimator with the smallest value of spatial resolution, for a given sensitivity. For this reason, this simplification of p(x,y,z) appears to be useful.

A similar situation occurs in optics where the point spread function of a lens is analogous to the psrf of a collimator. Here too, equations analogous to equation (10) are too complex for routine computation and comparison of

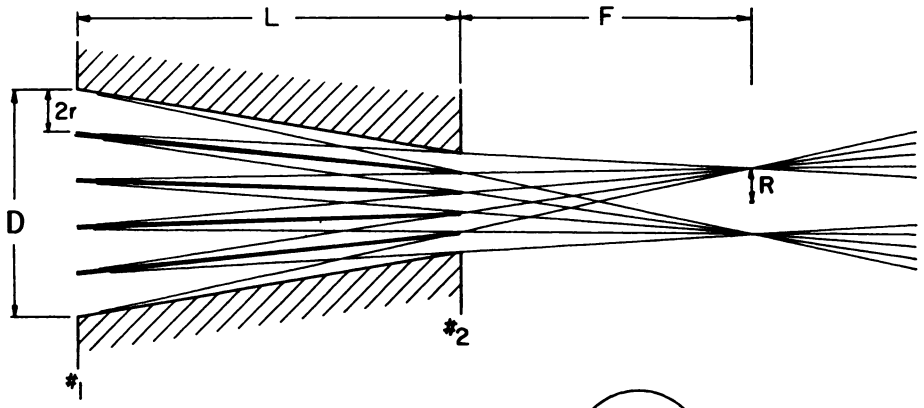

	b	h	2r
FACE #1	.471"	.407"	.451"
FACE #2	.202	.175	.193

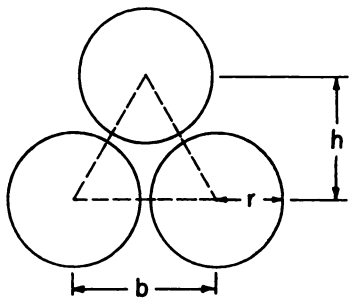

Fig. 3. Collimator designed for brain scanning with ^{99m}Tc. D = 2.33″, F = 3″, L = 4″, R = .34″; geometrical efficiency G = 2.87 × 10^{-3} cm^2. Despite thin septa, penetration is negligible for 140 keV γ-rays.

images produced by different lenses. To establish criteria for lens quality, several approaches have been taken. In keeping with the interest (among astronomers) in separating double stars, Lord Rayleigh (22) introduced the resolution concept called resolving power, which was defined in terms of the width of the point spread function or the Airy diffraction pattern (23). It was, however, recognized early that the lens which resolved point sources best did not always produce the best image of distributed objects. Accordingly, Foucalt (24) introduced, as test objects, line patterns consisting of sets of lines having a width equal to the spacing between them. The resolution or resolving power of a lens was then defined in terms of the smallest line spacing that could be seen in the image; e.g., a lens might have a resolving power of 100 lines/mm. Some form of this test is still the most widely used method for evaluating lenses (25).

While this criterion of lens quality is based on the response of a lens to a distributed source of illumination, it is nevertheless invalid to conclude that, if lens A has higher resolving power than lens B, then lens A will form a better image of an arbitrary object. This is because this measure of resolving power tells us something about how the lens will reproduce the small details or fine structure in the object, but nothing about how the large, coarse structure will be reproduced. In short, the intuitive notion that the lens which resolves small structures best will certainly resolve large structures best is not valid. In general, objects viewed by optical systems contain a wide range of structure sizes. Therefore it appears that a definition of resolution based on a measure of lens response as a function of structure size would be more useful than a single number to describe lens performance. In recent years, this generalization of resolving power has been intensively developed in optics and reviewed by Perrin (26). Since an almost identical formulation can be applied to scanning systems, this approach will be briefly described. [Here, $\sigma(x,y)$ is used to specify either the intensity distribution of light or radioactivity in the object, while $C(x,y)$ specifies either the light intensity or count rate forming the image.]

To clarify this alternative formulation of spatial resolution, we will draw an analogy between optical systems (or scanning systems) and the more familiar sound reproducing system.

It is well known among audiophiles, as well as engineers, that any sound, from a single note on the piano to the incredibly complex output of a full symphony orchestra, can in principle be described in terms of its Fourier spectrum; that is, the amplitude, phase, and frequency of the sine and cosine waves that must be superimposed to produce the sound. Somewhat less familiar is the fact that a two-dimensional object,[1] such as $\sigma(x,y)$, can be analyzed in terms of its spatial frequency components, measured in cycles/cm (sound is analyzed in terms of its temporal frequency components, measured in cycles/second). The fine structural details of $\sigma(x,y)$ require high frequency sine and cosine waves for their representation while the large, coarse structures require low frequency, long wave length components.

[1]We assume that the structures in $\sigma(x,y)$ are oriented in no special way, so that the frequency spectra along X and Y axes (in any orientation about the Z axis) are essentially the same; thus, the spectral analysis of $\sigma(x,y)$ need be treated in only one dimension.

To continue the analogy, the engineer must take into account the range of frequencies contained in the music that the audio system is to reproduce, and design a system having uniform or flat response over this range. Similarly, if the optical (or scanning) system is to form a perfect image of $\sigma(x,y)$, the system must respond to all frequencies in $\sigma(x,y)$ equally well; that is, the response must be flat over the band of frequencies required to represent the object, $\sigma(x,y)$, if its image, $C(x,y)$, is to be accurate.

This can be related to the discussion of contrast or modulation if σ_t and σ_0 in equation (4) are now thought of as the maximum and minimum amplitudes associated with a sinusoidal distribution of radioactivity having frequency ν, and C_t and C_0 in equation (5) are the corresponding count rates due to this frequency component. (Fig. 5.) The MTF(ν) is then just the spatial frequency response of the optical system (or the collimator-detector-pulse height analyzer of the scanning system); it tells us what fraction of the object contrast is transmitted by the system to appear as image contrast. It is important to note that the MTF(ν) is not a single number, but a function of space frequency, ν. This means that we have in the MTF(ν) a measure of the detector response to simple structures (sinusoidal distributions) of all sizes. The response to a complex structure is simply the sum of responses to its frequency components.

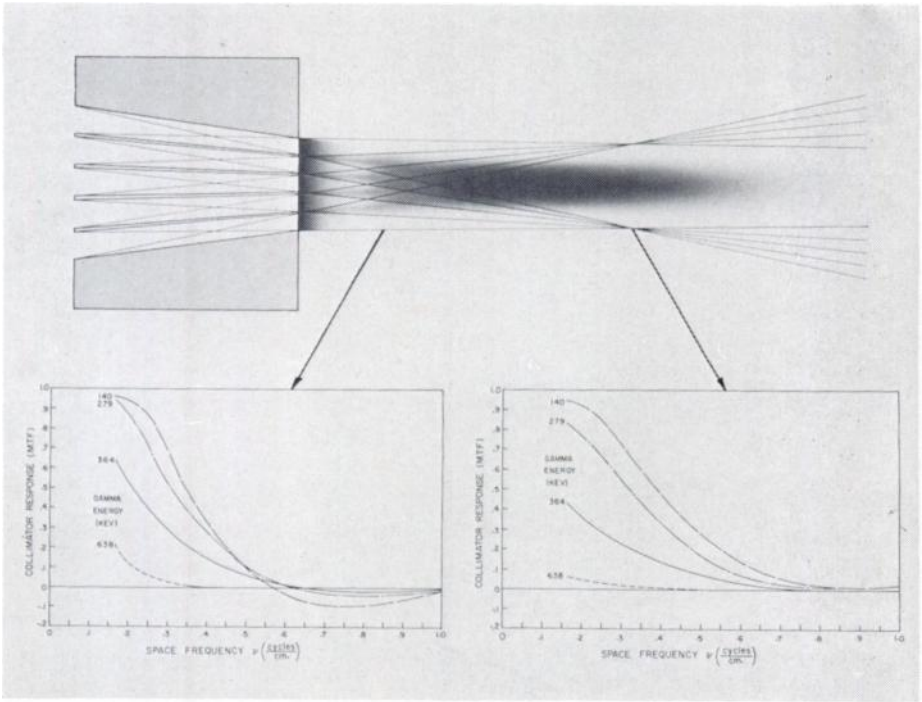

Fig. 4. Collimator designed for ^{203}Hg (279 keV). If sensitivity is associated with exposure density within the collimator field of view, the upper figure illustrates the "geometrical" response to a point source. The spatial frequency response (MTF) is plotted below for several γ energies. The decrease in MTF with increasing γ energy is equivalent to a decrease in contrast, due to increasing septal penetration.

In view of this consideration, it would be desirable to design imaging systems so as to make the MTF(ν) as near 1 as possible for the entire range of frequencies contained in $\sigma(x,y)$. In practice, this is never achieved for scanning systems because the MTF can be made large only by making the collimator field of view small;[1] unfortunately, this is accompanied by a sharp decrease in collimator efficiency, and therefore by an increase in random, statistical structure. For this reason, it is always necessary to compromise between the magnitude of the MTF and counting efficiency (or between resolution and sensitivity).

Although the MTF(ν) is more complex than the usual definition of resolution, it has the advantage that, once it is determined, we can find the image, C(x,y), of a given object, $\sigma(x,y)$, by summing the responses to the frequency components in the object. In principle, it is possible to compute the MTF from the theoretical point source response function, $p(x,y,z) = \Omega(x,y,z)/4\pi$. Since $\Omega(x,y,z)$ is a rather complex function for a multichannel focused collimator, it is more convenient to determine the MTF experimentally.

There are two simple methods for doing this. The most direct and intuitively clear is to observe (1), the response to a sinusoidal source of radioactivity, such as the one scanned for Figure 7. In such a source $\sigma_o = 0$, so that $m_o = 1$ in equation (4). In this special case, the MTF $= m_i = \frac{C_t - C_o}{C_t + C_o}$. This is analogous to measuring the frequency response of an audio amplifier by observing its response to a sine wave input signal. Alternatively (2), if the line spread function, L(x) (the response to a line source of radioactivity parallel to the Y-axis) is observed, the MTF can be found (26-28) by taking the Fourier transform of L(x).

If a source of low energy γ-rays is used in either of these procedures, the resultant MTF reflects, primarily, the smoothing effect due to the finite width of the collimator field of view. If γ's of higher energy are used, so that septum penetration is not negligible, then the resultant MTF reflects the effects of both geometrical and penetration responses. (Fig. 4.) If, in addition, the measurments of C_t and C_o are made with the source imbedded in a scattering medium, the effect of scattered radiation on MTF is also observed. Thus, by proper choice of γ energy and surrounding medium, the MTF can be used as a measure of the reduction in contrast due to a combination of background, penetration, scatter and finite collimator resolution. Since, in the special case when $m_o = 1$, as in method (1) above, the MTF $= m_i$, the relationship between MTF and P,S, and B is given by equation (9).

In terms of its complexity and generality, the MTF (ν,z) of a detector stands between the point of source response function, p(x,y,z), and the resolving power measured by any single number. While this level of analysis has recently been

---

[1]For MTF $\cong$ 1 at frequency ν, it is necessary that the collimator field of view be small compared to one-half wave length; e.g., for ν = 1 cycle/cm, $\frac{\lambda}{2}$ = .5 cm and the diameter of view must be much smaller than .5 cm for MTF to be near 1 at this spatial frequency.

seen as a "breakthrough" in optics, there is some doubt, at this time, whether the added complexity is justified, for radioisotope imaging systems, by the increased generality of the description. Although it is generally agreed that any single number used to measure spatial resolution at a given distance must be somewhat less adequate than a one-dimensional function such as the MTF(ν), Brownell (29) has pointed out that the psrf's of properly designed focused collimators have approximately Gaussian shapes (and in any case are less bizarre than the corresponding point spread functions of some lenses), and may therefore be replaced by a single number that measures the resolution.

C. *Spot Structure:* There is quite general agreement that every collimated γ-ray should be recorded by the imaging system, but there is little concensus as to how this should be done. Most systems produce some kind of mark or spot on recording paper or film for each detected γ: for example, tiny dots, discs, circles, crescents, lines, rectangles, triangles, asterisks, letters, numerals, etc. Clearly none of these marks bears any intrinsic relation to the distribution of activity or the imaging properties of the system, and in this sense they introduce artificial "spot structure."

This artifact is reduced by recording a bell-shaped spot on film, which tends to duplicate the position information given by the collimator. (Fig. 6.) In contrast, the recording of a tiny dot at a position corresponding to the collimator axis amounts to replacing p(x,y,z) by its most probable value, and thereby introducing distortion.

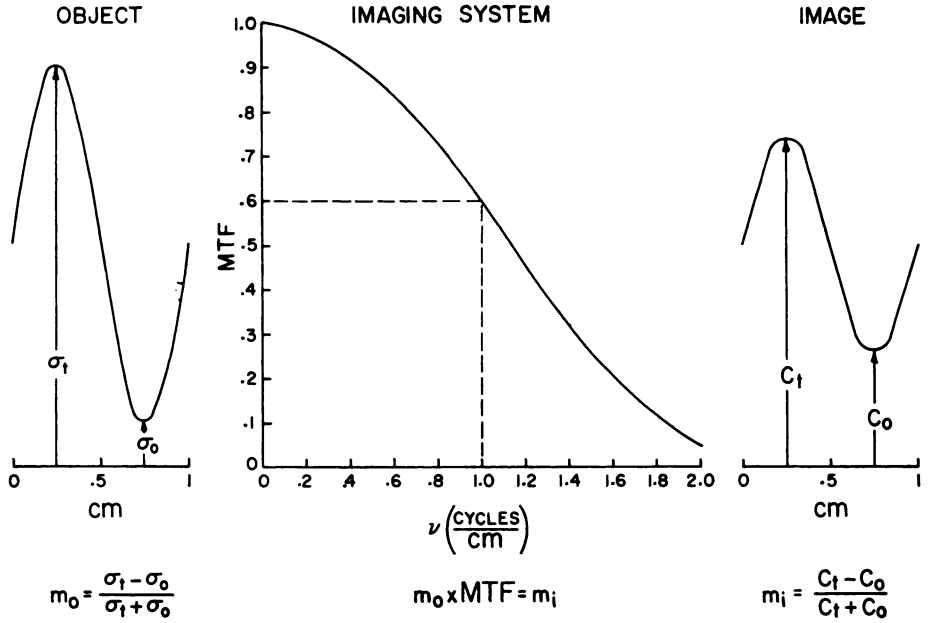

Fig. 5. If the distribution of radioactivity (Object) and the output (Image) are described in terms of their space frequency components, the scanner (Imaging System) can be described in terms of its frequency response or Modulation Transfer Function. The MTF can be used as a generalized definition of spatial resolution.

Experiments have been performed in which γ pulses from a single detector were recorded on film by two pulsed light projectors producing spots of different sizes. (Fig. 7.) Subjective evaluations of these photoscans tend strongly to favor ½" diameter bell-shaped spots over smaller spots that are either bell-shaped or sharply defined. Larger spots have not yet been tried. Thus, we have not carried this notion so far as to produce bell-shaped spots that are as large as the collimator field of view (which was ¼" diameter for the photoscans shown in Figure 7). A further rationale for doing so has been discussed by Morgan (30). If a tiny dot is recorded for each detected γ-ray, then the high frequency response (and the bandwidth) of the recording system greatly exceeds that of the collimated detector. Since the noise in a system increases with bandwidth, high frequency noise is introduced and recorded by such a system. If, on the other hand, the bandwidth of the recording system is matched to that of the detector, a minimum of noise is introduced by the recording system. This match can be achieved, approximately, by recording a spot that resembles in size and shape the point source response function of the collimator. (Since the shape of the

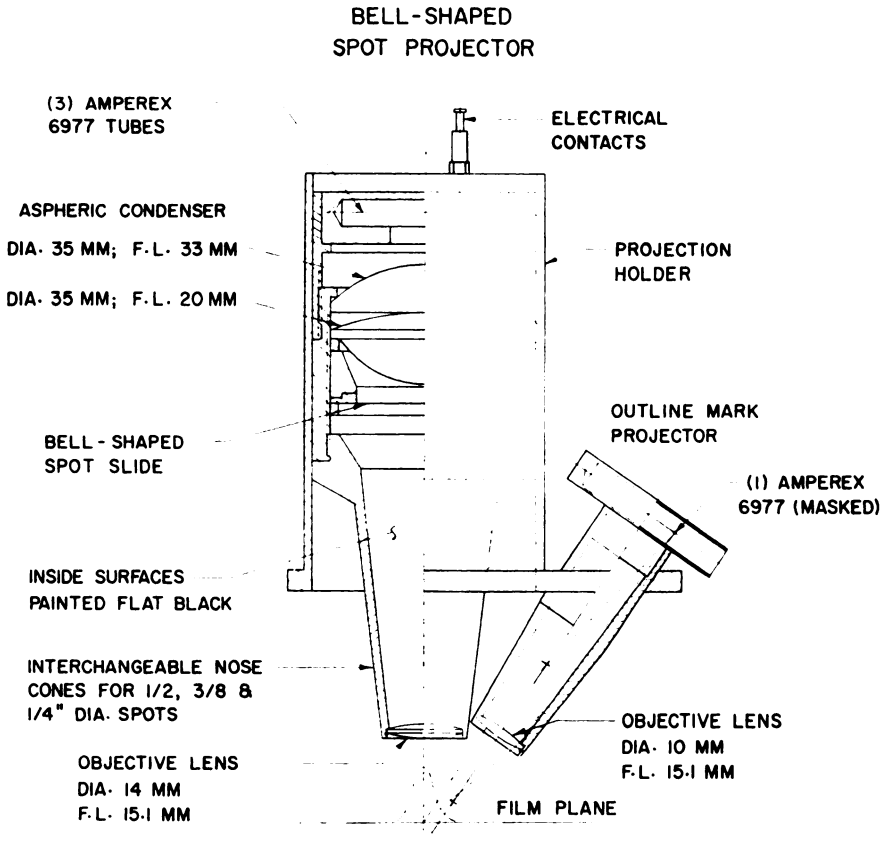

Fig. 6. For each detector, there is (1) a pulsed light projector which produces a bell-shaped spot on film for each detected γ-ray and (2) an outline mark projector. The size of the projected bell-shaped spot can be controlled.

psrf varies with distance from the collimator, an average shape might be used.)

Morgan and Tuddenham (31) have pointed out that a mismatch of bandwidths of the detector and recorder is especially serious because the bandwith of the human eye is even greater than that of the recorder; consequently, recorder noise might disturb the visualization of important structures in the photoscan. This can be overcome to some extent by viewing the photoscan from a distance so great that the eye cannot resolve the high frequency noise.

To summarize this point of view, we can say first, that the spatial frequency response, or MTF(ν), of the collimated detector should be made as close to 1 as possible over the band of frequencies contained in the structures of $\sigma(x,y)$ which are to be detected; second, that the bandpass of the recording system should be matched to that of the detector; and third, that the resultant image should be so viewed that the structures to be detected appear on the retina under optimal conditions for visual perception [one such condition being that the structure have a fundamental frequency of approximately 10 cycles, or line pairs, per millimeter on the retina (32)].

In addition to these considerations, the smooth image (Fig. 8) that is formed by overlapping bell-shaped spots is ideal for contrast enhancement on closed circuit television (33), for isocount contour plotting (34,35) (Fig. 9) or for similar manipulations with a flying spot scanner (36).

In the brain scanner, for each detector there is a pulsed light projector (Fig. 6), resembling a slide projector in miniature, which produces a spot on film for each γ pulse selected by the associated PHA. In each projector, the light source consists of three Amperex 6977 triode indicator tubes operated in parallel. The green phosphor on the plate of this tube appears to have a decay time of approximately 5 μ sec as measured with a photomultiplier having an S11 photocathode. Hence, the light per pulse is essentially constant over a very wide range of count rates. Different pulse lengths may be selected to provide a useful range of film densities. The slide that is projected is a disc which is nearly transparent at the center and opaque at the edges, its density varying smoothly between these extremes. When this is projected, the light intensity on the film has a bell-shaped distribution. The diameter of this projected image can be set at ½", ⅜" or ¼" by choice of the objective lens position relative to the slide and film. The four light projectors are oriented with respect to the two sheets of film in the same manner as the four scintillation detectors are oriented with respect to the patient's head. The projectors travel with the scan mechanism by means of a rigid mechanical connection.

D. *Line Structure:* Perhaps the most prominent artifact in photoscans (as in television) is line structure caused by the relatively large spacing between scan lines. To reduce this artifact, we have used a line spacing of 1/16" in most scans, with five multiples of this value available. When a ½" bell-shaped spot is recorded for each γ-ray, no line structure is evident. However, reduced line spacing tends, indirectly, to aggravate the following two artifacts:

E. *Variable Line Spacing:* If the space between scan lines varies, the number of counts recorded per unit area varies inversely, introducing an apparent variation in the concentration of activity. If the line spacing is so close that the spacing variation is not evident, there is danger of interpreting a variation in the number of counts per unit area due to spacing variation as a variation in concentration.

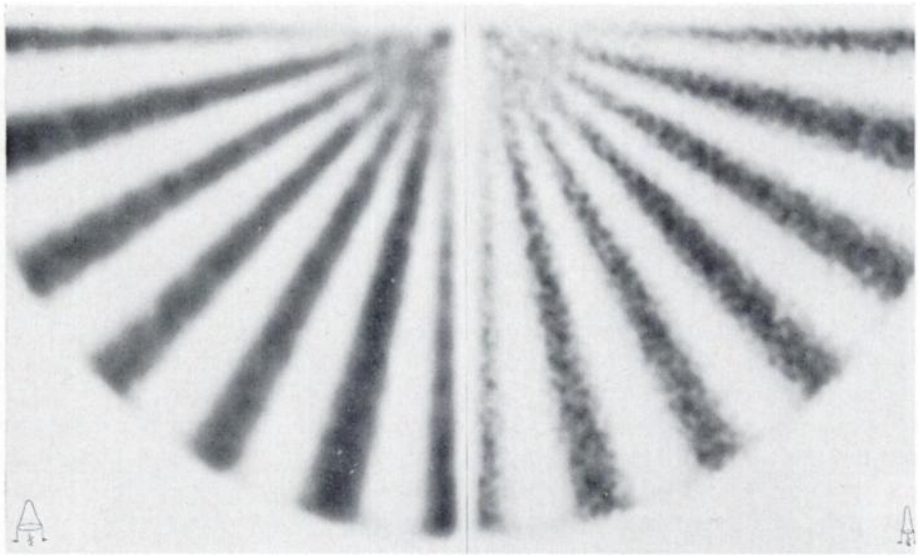

Fig. 7. Here a sunburst pattern containing radioactivity in which the concentration at a fixed radius varies sinusoidally, is scanned by a single detector. Each detected γ-ray pulses two spot projectors which produce bell-shaped spots of ½″ diameter (Left) and ¼″ diameter (Right). The ½″ spots reduce the high frequency response of the recording system to more nearly match that of the detector.

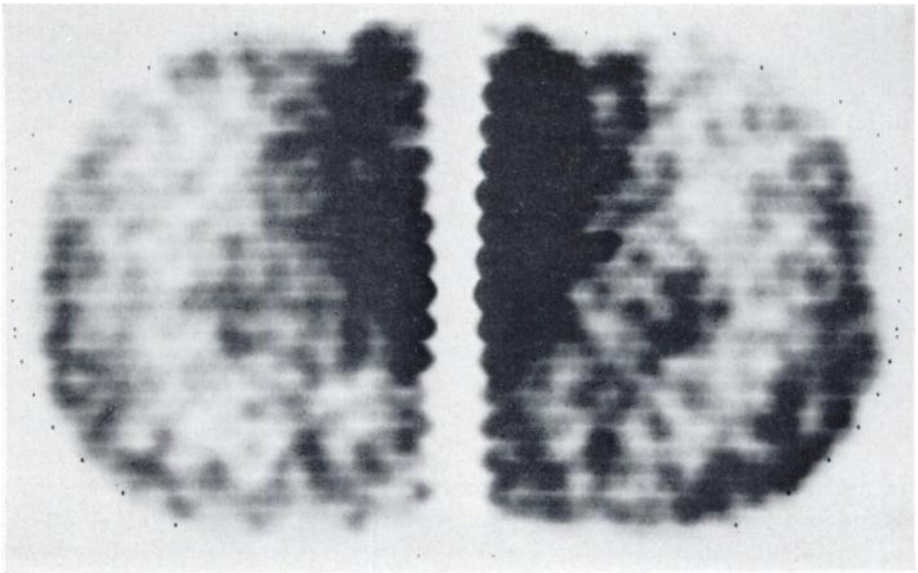

Fig. 8a. Simultaneous lateral scans made in 85 sec. showing a midline lesion. Scan was begun 10 minutes after intravenous injection of 10 mCi of ^{99m}Tc as $(TcO_4)^-$. Scan speed, 2″ per sec.; index ¼″. Such rapid scans are made only under emergency conditions.

In the ACRH brain scanner, the line spacing is determined by the rotation of the indexing screw, rather than by the time during which the indexing motor is turned on. Thus, variations in the loading of the indexing motor do not affect the line spacing. In addition, the accumulation of spacing errors is minimized.

In this system, ball screws are used for both X and Y motions, and one complete rotation of the index screw produces a vertical travel of ¼". A cam with four detents, mounted on the index screw, operates a microswitch to determine the 1/16" line spacing.

F. *Scalloping:* Another consequence of reduced line spacing is the need for greater scan speed if the same area is to be covered in the same time. If the recording system employs any form of integrating circuitry that has a response time much greater than the mean time between pulses (such as count rate meter circuitry used for background erase of contrast enhancement), then structures detected in the object are displaced in the image in the direction of scan motion. Since the direction of motion changes on alternate lines, his displacement alternates, creating scalloping. Inasmuch as the displacement is proportional to scan speed, scalloping is aggravated by increased speed. This artifact is eliminated in the ACRH scanner since no integrating circuitry is used in the recording system. When the low energy detectors and light weight shields were installed, scan speeds were doubled, so that speeds of 2, 1.3, .9, .6, and .4 inches per second are available. Scan speed is monitored by a generator-tachometer.

G. *Variable Scan Speed:* A variation in scan speed is indistinguishable from a change in count rate. For this reason, it is essential that the fractional variation in scan speed be negligible compared to the minimum fractional change to be detected in the count rate. In the present system, scan speed is held constant ± 1% by means of a feedback system that incorporates a magnetic amplifier. Even so, some structure due to variations in scan speed can be detected when regularly space timing pulses are recorded.

H. *Non-equilibrium:* If the distribution of activity changes during the scan period, the image does not represent an equilibrium state. This is especially noticeable in the ACRH system where the first scan line made by the upper detectors is adjacent to the last line of the lower detectors. Since the time between these lines is usually about 10 minutes, any change in the distribution during this time is apparent. It has been found that this artifact is negligible when the scan is begun about 10 minutes after injection of ^{99m}Tc as pertechnetate.

I. *Patient Motion:* A common cause of distortion in the image is motion of the patient during the scan. This is less likely to occur if the scan time is short and the patient is comfortable. In the present system, the patient reclines on a modified operating table (Fig. 1) which can be contoured in a variety of ways and which has padded arm and back rests that are adjustable. In addition, the head is held in a comfortable sling of flexible, transparent plastic sheet which is supported by two rods that can be rotated to elevate and turn the head.

To summarize, we have attempted to reduce scanning artifacts wherever

possible. This goal has necessitated the elimination of any form of data manipulation that depends on circuitry having a time lag, such as a count rate meter. It is felt that these manipulations (contrast enhancement, background erase, etc.) are best performed on the undistorted[1] photoscan by means of closed circuit television or a flying spot scanning system.

SPECIAL FEATURES

A. *Calibration System:* Ordinarily, no quantitative information is available from a photoscan, and in order to obtain such information, it is necessary to have some way of relating film density to count rate. For this purpose, it is convenient to record on the photscan a wide range of known count rates under the same conditions (scan speed, index width, spot intensity, etc.) used to perform the scan. This can be accomplished by using a simple random count generator consisting of a radioactive source and detector. The mean count rate can be varied by introducing a calibrated absorber between the source and detector. The calibration system installed in the brain scanner (Fig. 10) consists of a ^{204}Tl source and a Geiger tube detector. (Thallium-204 emits a .765 MeV β^--ray, no γ-rays, and has a 4.1 year half-life.)

[1]A form of background erase that does not make use of circuitry having a time lag is actually available, and used, in this system. By using a suitably short pulse length to the light projectors, it is possible to require any number of pulses to be present before the film density exceeds the fog level. This technique makes use of the non-linear response of the film rather than a time dependent non-linearity in the electronic circuitry.

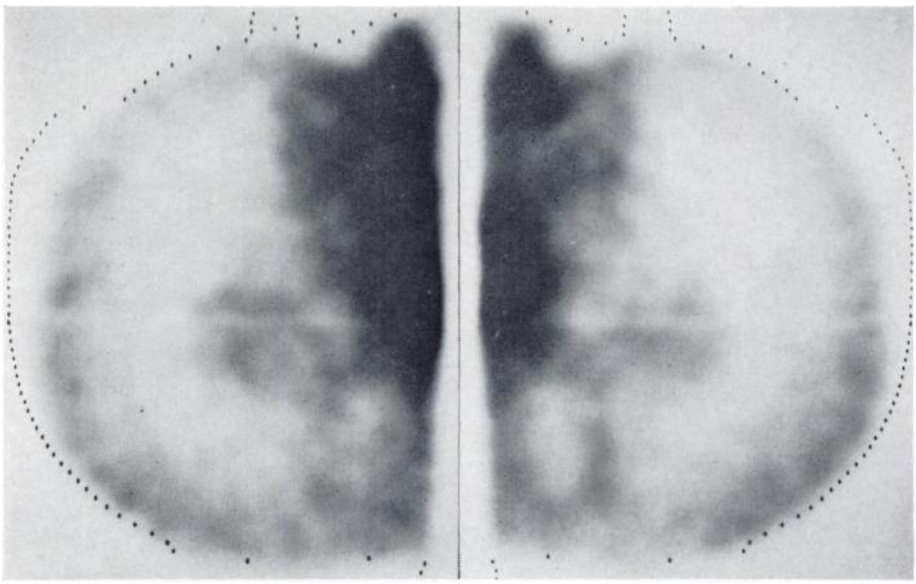

Fig. 8b. Routine simultaneous lateral scans made in 10 minutes show the midline lesion in somewhat more detail. Scan was begun immediately after completion of 8a. Scan speed, 0.9″ per sec.; index 1/16″. Collimators illustrated in Fig. 3 were used.

The source is contained in a polyethylene tube located behind a slit collimator that has an adjustable width for calibration and to compensate for decay. The Geiger tube is mounted behind a slit collimator of fixed width. The effective slit length, hence the count rate, is determined by the position of an absorber, which is attached to the scan mechanism and moves horizontally between the source and detector collimators. The .765 MeV β^--rays are completely absorbed in a $\frac{1}{32}$" Al sheet which is backed by a $\frac{1}{16}$" Pb sheet to attenuate low energy bremsstrahlung produced in the Al. Another Al sheet covers the lead to provide a better working surface. This sandwich of Al-Pb-Al sheets is held together by epoxy. The height of this absorber changes in 26 steps, each altering the count rate by 20% with respect to adjacent steps. As the scanner moves between its limits of horizontal motion (12"), the count rate changes from 100 counts per minute to 9,500 counts per minute during the 26 steps of 20% increase. Pulses from this system are fed to the spot projectors to produce a calibrated wedge for each detector channel. The count rate at any point on the patient's head can then be determined by matching the film density at that point with the corresponding film density on the calibrated step wedge. Photoscans and calibrated step wedges are recorded on two sheets of Royal Blue x-ray film. The film is held in x-ray cassettes in which the aluminum entrance windows have been replaced by $\frac{1}{8}$" sheets of tempered glass and removable, optically opaque, cover slides. The film is processed in a Kodak X-O-Mat to insure uniformity of development.

B. *Patient and Scan Information Recording System:* For each scan, the operator fills out an information form that identifies the patient and specifies the conditions under which the scan was performed. (Quantity, chemical form, and time of injected activity, scan time, speed, index, collimator, spot size, are recorded, as well as other data and remarks that might be relevant to the interpretation of the photoscan.) A dual channel optical system records a reduced but readable image of this form on each sheet of film and simultaneously marks one film LEFT, the other RIGHT, corresponding to the left and right sides of the patient's head. This system has virtually eliminated the problem of labeling and identifying the film.

C. *Film Format:* While the photoscans are recorded on 14" × 17" film, the horizontal motion is limited to 12", leaving a two-inch strip of film to record the information form described above. The vertical motion is also limited to 12", but since the upper and lower detectors are separated by 4½", the total area covered is 12" by 16½". The upper and lower 1" strips are used to record the calibration step wedges for the upper and lower detectors, respectively. This leaves an area 12" by 14½" in which the brain scan can be recorded.

D. *Scan Control System:* Two modes of scanning are possible, namely, Profile Scanning and Rectangular Scanning. In profile scanning, the vertical indexing and horizontal scan reversal are accomplished by the interrupted light beam mentioned earlier. In rectangular scanning, adjustable limit bars define the region to be scanned. Microswitches, actuated by a control rod carried by the detectors and operating within this rectangle, index the detectors vertically and reverse the horizontal scan direction. Panel lights indicate failure of the microswitches, in which case the system will scan another .080" before actuating a "backup" microswitch that reverses the scan direction.

E. *Electronic Circuits:* The circuits comprising the ACRH brain scanner employ semiconductor components wherever possible. Silicon controlled rectifiers are used as power switches in the horizontal and vertical drive systems to eliminate switch contact noise. All circuits for the detection, analysis, and recording of γ-ray signals, including those used for calibration, are transistorized. These circuits are built into small plug-in units and have proven to be remarkably stable and trouble-free.

F. *Modifications Under Way:* While maintaining a certain skepticism concerning the efficacy of a "Universal Scanner," the success of ^{99m}Tc in applications other than brain scanning (11-14), has led us to modify the ACRH scanner for more general use with low energy isotopes. In addition to the modifications of the detectors and shields which have already been mentioned, these units have been set on movable carriages that permit the distance between collimator faces to be adjusted from 8″ to 14½″. A sliding couch is under construction which will allow the head, neck or torso of the patient (lying on his side) to be placed between the detectors. In this way we hope to use the system for thyroid scanning (with one detector), for kidney scanning (with two detectors), and for lung and liver scanning (with all four detectors).

RESULTS AND CONCLUSIONS

Between August, 1963 and the present date, this system has been used with ^{99m}Tc to scan approximately 800 patients. The clinical procedure and findings have been reported in detail elsewhere (37). Figure 11 summarizes an analysis of the first 182 scans.

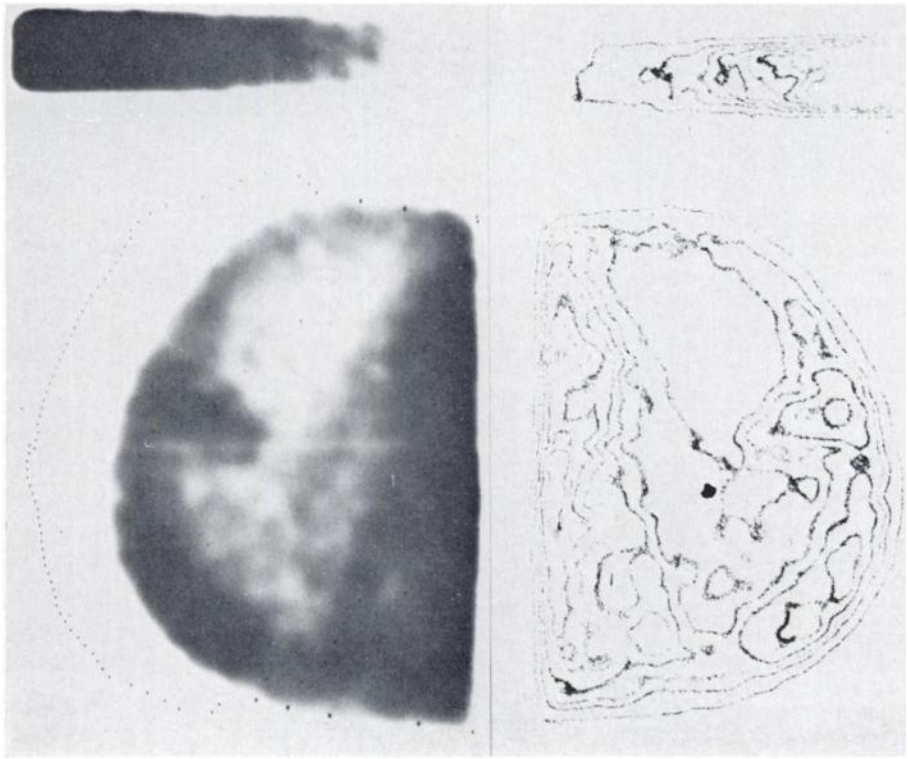

Fig. 9. The count rate at any point on the brain scan can be determined by matching the film density at that point to a density on the calibrated wedge of known count rates. Quantitative measurement of count rates may be facilitated by plotting isocount contour lines of the brain scan and calibrated wedge.

Although the present system was designed primarily for brain scanning, it is felt that many of the techniques incorporated in this device will be helpful in other scanning applications. Modifications of this system are being made which will allow us to investigate these possibilities.

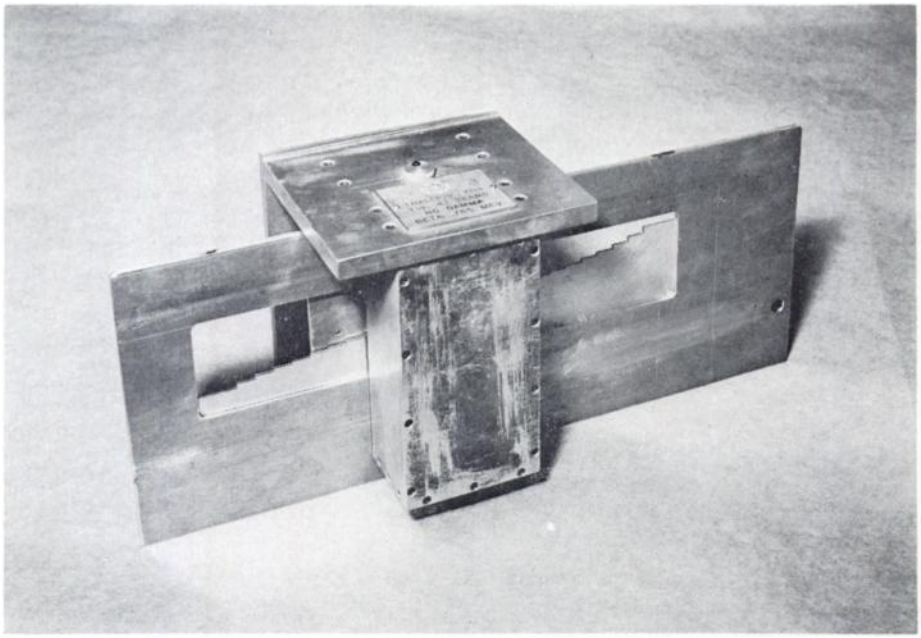

Fig. 10. The calibration wedge generator consists of a line source of ^{204}Tl and a Geiger tube separated by a step wedge absorber to produce random count rates which cover the range of 100 to 9500 counts per minute in 26 steps of 20% increase as the absorber is moved through the 12″ horizontal scan motion.

ACKNOWLEDGMENT

We are especially grateful to John J. Stupka, Charles R. Brebach and Bernard W. Fromes for innumerable ideas and complete cooperation in every aspect of the mechanical design and construction, and to Alexander Sinila for his essential contribution to the detector transport design. In addition, Rosa Lee Seslar, Violet Stark, Vivienne Reynolds and Joan Anderson performed the brain scans with great care.

REFERENCES

1. Cassen, B., Curtis, L., Reed, C., Libby, R.: Instrumentation for ^{131}I Use in Medical Studies, *Nucleonics* **9(2)**: (1951).

2. Brownell, G. L., and Sweet, W. H.: Localization of Brain Tumors with Positron Emitters. *Nucleonics II*, **40(11)**: (1953).

3. Anger, H. O.: Scintillation Camera. *Rev. Sci. Instr.* **29**:27 (1958).

4. Cassen, B.: Theory of Scanning and Imaging of Radioisotope Distributions. In *Medical Radioisotope Scanning*, Volume 1, Vienna, IAEA (1964), p. 77.

5. Kuhl, D. E.: A Clinical Radioisotope Scanner for Cylindrical and Section Scanning. In *Medical Radioisotope Scanning*, Volume 1, Vienna, IAEA (1964), p. 273.

6. ANGER, H. O.: Gamma-Ray and Positron Scintillation Camera. *Nucleonics* **21(10)**:56 (1963).

7. BENDER, M. A.: The Digital Autofluoroscope. In *Medical Radioisotope Scanning*, Volume 1, Vienna, IAEA (1964), p. 391.

8. KELLERSHOHN, D., LANSIART, A., ET DESGREZ, A.: Deux nouveux types de detecteur pour camera a rayons X ou γ. In *Medical Radioisotope Scanning*, Volume 1, Vienna, IAEA (1964), p. 333.

9. TER-POGOSSIAN, M. M. AND EICHLING, J. D.: Autofluorography with an X-ray Image Amplifier. In *Medical Radioisotope Scanning*, Volume I, Vienna, IAEA (1964), p. 411.

10. BECK, R. N.: A Theoretical Evaluation of Brain Scanning Systems. *J. Nucl. Med.*, **2**:314 (1961).

11. HARPER, P. V., BECK, R. N., CHARLESTON, D. B., AND LATHROP, K. A.: Optimization of a Scanning Method Using ^{99m}Tc. *Nucleonics* **22(1)**:50, January (1964).

12. BECK, R. N. AND SCHUH, M. W.: Quantitative Evaluation of Scintillation Detector Response to Scattered Radiation. To be published.

13. HARPER, P. V., LATHROP, K. A., ANDROS, G., MCCARDLE, R., GOODMAN, A., BECK, R. N., AND COVELL, J.: Technetium 99m as a Clinical Tracer Material. In *Radioaktive Isotope in Klinik Und Forschung*, **6**:136-145 (1965).

14. HARPER, P. V., LATHROP, K. A., JIMINEZ, F., FINK, R., AND GOTTSCHALK, A.: Technetium 99m as a Scanning Agent. *Radiology* **85**:101-108 (1965).

15. BECK, R. N. AND CHARLESTON, D. B.: A Small Animal Scanner. *Intern. J. Appl. Radiation Isotopes*, **15**:101 (1964).

16. HARPER, P. V.: A 3-D Viewing System. In *Proceedings of a Symposium on Fundamental Problems in Radioisotope Scanning*, Chicago, Illinois, 8-9 May, 1965, edited by A. Gottschalk and R. N. Beck. To be published by Charles C Thomas Publishers, Springfield, Illinois.

17. GOTTSCHALK, A. AND BECK, R. N. (Eds.) *Proceedings of a Symposium on Fundamental Problems in Radioisotope Scanning*, Chicago, Illinois, 8-9 May, 1965. To be published by Charles C Thomas Publishers, Springfield, Illinois.

18. BECK, R. N.: Collimators for Radioisotope Scanning Systems. In *Medical Radioisotope Scanning*, Volume 1, Vienna, IAEA (1964), p. 211.

19. BROWNELL, G. L.: Theory of Radioisotope Scanning. In *Medical Radioisotope Scanning*, Volume 1, Vienna, IAEA (1964), p. 3.

20. ROSSMANN, K.: Detail Visibility in the Presence of Quantum Fluctuation. In *Proceedings of a Symposium on Fundamental Problems in Radioisotope Scanning*, Chicago, Illinois, 8-9 May, 1965, edited by A. Gottschalk and R. N. Beck. To be published by Charles C Thomas Publishers, Springfield, Illinois.

21. BECK, R. N.: A Theory of Radioisotope Scanning Systems. In *Medical Radioisotope Scanning*, Volume 1, Vienna, IAEA (1964), pp. 35-56.

22. LORD RAYLEIGH: Investigations in Optics, with Special Reference to the Spectroscope. In *Scientific Papers*, Volume 1, Cambridge University Press (1899), p. 420.

23. AIRY, G. B.: On the Diffraction of an Object with Circular Aperture. Trans. Cambridge Phil. Soc. **5**:283-290 (1835).

24. FOUCALT, L.: Memoire sur la Construction des Telescopes en Verre Argente. *Ann. de l'Observatoire Imp. de Paris* **5**:197-237 (1859).

25. WASHER, F. E. AND GARDNER, I. C.: Method for Determining the Resolving Power of Photographic Lenses. National Bureau of Standards Circular 533 (1953).

26. PERRIN, F. H.: Methods of Appraising Photographic Systems. *J. Soc. Motion Picture and Television Eng.* **69**:151-156, March; 239-249, April (1960).

27. MOZLEY, J. M.: Modulation Transfer Function for Radioisotope Scanners. In *Proceedings of a Symposium on Fundamental Problems in Radioisotope Scanning*, Chicago, Illinois, 8-9 May, 1965, edited by A. Gottschalk and R. N. Beck. To be published by Charles C Thomas Publishers, Springfield, Illinois.

28. BECK, R. N.: The Radioisotope Imaging System as a Whole: General Considerations. In *Proceedings of a Symposium on Fundamental Problems in Radioisotope Scanning*, Chicago, Illinois, 8-9 May, 1965, edited by A. Gottschalk and R. N. Beck. To be published by Charles C Thomas Publishers, Springfield, Illinois.

29. BROWNELL, G. L.: Spatial Resolution. In *Proceedings of a Symposium on Fundamental Problems in Radioisotope Scanning,* Chicago, Illinois, 8-9 May, 1965, edited by A. Gottschalk and R. N. Beck. To be published by Charles C Thomas Publishers, Springfield Illinois.

30. MORGAN, R. H.: Summary Remarks. In *Proceedings of a Symposium on Fundamental Problems in Radioisotope Scanning,* Chicago, Illinois, 8-9 May, 1965, edited by A. Gottschalk and R. N. Beck. To be published by Charles C Thomas Publishers, Springfield, Illinois.

31. TUDDENHAM, W. J.: Density Gradient and the Significance of the Image Edge. In *Proceedings of a Symposium on Fundamental Problems in Radioisotope Scanning,* Chicago, Illinois, 8-9 May, 1965, edited by A. Gottschalk and R. N. Beck. To be published by Charles C Thomas Publishers, Springfield, Illinois.

32. DEPALMA, J. J. AND LOWRY, E. M.: Sine-Wave Response of the Visual System. II. Sine-Wave and Square-Wave Contrast Sensitivity. *J. Opt. Sco. Am.* **52**(3):328-335 (1962).

33. BENDER, M. A. AND BLAU, M.: Photoscanning. In *Medical Radioisotope Scanning,* Vienna, IAEA and WHO (1959), p. 31.

34. CHARLESTON, D. B., BECK, R. N., EIDELBERG, P. AND SCHUH, M. W.: Techniques Which Aid in Quantitative Interpretation of Scan Data. In *Medical Radioisotope Scanning,* Volume 1, Vienna, IAEA (1964), pp. 509-525.

35. CHARLESTON, D. B.: An Analog Approach to Scan Readout Data Manipulation and Enhancement. In *Proceedings of a Symposium on Fundamental Problems in Radioisotope Scanning,* Chicago, Illinois, 8-9 May, 1965, edited by A. Gottschalk and R. N. Beck. To be published by Charles C Thomas Publishers, Springfield, Illinois.

36. KOUVANAZY, L. S. G. AND JOSEPH, H. M.: Image Processing, *Proc. Inst. Radio Engineers* **43**(5):560 (1955).

37. HARPER, P. V., FINK, R. A., BECK, R. N., CHARLESTON, D. B., LATHROP, K. A., AND EVANS, J. P.: Rapid Brain Scanning with ^{99m}Tc. VII Symposium Neuroradiologicum, New York, N. Y., 20-25 September, 1964. To be published in Acta Radiologica.

Announcement to Authors

Preliminary Notes

Space will be reserved in each issue of THE JOURNAL OF NUCLEAR MEDICINE for the publication of one preliminary note concerning new original work that is an important contribution in Nuclear Medicine.

Selection of the preliminary note shall be on a competitive basis for each issue. One will be selected after careful screening and review by the Editors. Those not selected will be returned immediately to the authors without criticism. Authors may resubmit a rejected or revised preliminary note for consideration for publication in a later issue. The subject material of all rejected manuscripts will be considered confidential.

The text of the manuscript should not exceed 1200 words. Either two illustrations, two tables, or one illustration and one table will be permitted. An additional 400 words of text may be submitted if no tables or illustrations are required. Only the minimum number of references should be cited.

Manuscripts should be mailed to the Editor, Dr. George E. Thoma, St. Louis University Medical Center, 1402 South Grand Blvd., St. Louis, Missouri 63104. They must be received before the first day of the month preceding the publication month of the next issue, *e.g.,* preliminary notes to be considered for the October 1967 issue must be in the hands of the Editor before September 1, 1967.